Research Square

Preprints are preliminary reports that have not undergone peer review.
They should not be considered conclusive, used to inform clinical practice,
or referenced by the media as validated information.

Dual TERT Promoter Mutations in Glioblastoma, IDH-Wildtype: A Case Report with Preclinical Investigations

Yohei Miyake
Yokohama City University: Yokohama Shiritsu Daigaku
Kensuke Tateishi
ktate12@yokohama-cu.ac.jp
Yokohama City University, Graduate School of Medicine https://orcid.org/0000-0001-6895-9013
Hinako Okagawa
Yokohama City University: Yokohama Shiritsu Daigaku
Akihide Koyama
Niigata University: Niigata Daigaku
Emi Hirata
Yokohama Shiritsu Daigaku
Kanoko Sasaoka
Yokohama City University: Yokohama Shiritsu Daigaku
Shuna Saito
Yokohama City University: Yokohama Shiritsu Daigaku
Shuto Fushimi
Yokohama City University: Yokohama Shiritsu Daigaku
Manabu Natsumeda
Niigata University: Niigata Daigaku
Erika Muraoka
Yokohama City University: Yokohama Shiritsu Daigaku
Shoji Yamanaka
Yokohama City University: Yokohama Shiritsu Daigaku
Satoshi Fujii
Yokohama City University: Yokohama Shiritsu Daigaku
Tetsuya Yamamoto
Yokohama City University: Yokohama Shiritsu Daigaku

Research Article

Keywords: Dual TERT promoter mutations, subclone, patient-derived xenograft model

Posted Date: March 8th, 2026

DOI: https://doi.org/10.21203/rs.3.rs-8931482/v1

License: This work is licensed under a Creative Commons Attribution 4.0 International License.
Read Full License

Version of Record: A version of this preprint was published at Brain Tumor Pathology on May 21st, 2026. See the published version at https://doi.org/10.1007/s10014-026-00540-8.

Abstract

Telomerase reverse transcriptase promoter (*TERT*p) mutations c.-124C > T (C228T) and c.-146C > T (C250T) are the most frequent single-nucleotide variants promoting telomerase activation in glioblastoma. Here, we describe a rare case of glioblastoma *IDH*-wildtype with dual *TERT*p mutations. Genomic analyses of multiregional tumor samples revealed co-occurring *TERT* C228T and C250T mutations across tumor regions, with variable copy number alterations of *EGFR* and *CDKN2A*. Notably, only the *TERT*p C228T mutation was retained in the corresponding patient-derived xenograft, accompanied by more extensive copy number alterations, implying a selective growth advantage for the *TERT* C228T-harboring subclone during tumor propagation in this case. These findings suggest that dual *TERT*p mutations may arise through subclonal evolutionary processes in glioblastoma and highlight telomere maintenance as a dynamic, heterogeneous process rather than invariably representing a fixed early oncogenic event.

Introduction

Glioblastoma, *IDH*-wildtype (GBM) remains one of the most lethal malignancies, and despite standard-of-care treatments, the median overall survival is less than two years [1]. Large-scale genomic analyses have demonstrated that deregulation of the RB, p53, and RTK/RAS/PI3K signaling pathways is an essential oncogenic event, and these alterations are considered to constitute the core mechanisms underlying GBM pathogenesis [2]. Consistently, experimental mouse models have shown that genetic alterations in related genes, including *Nf1, Egfr, Cdkn2a, Pten*, and *Trp53*, promote tumor formation, demonstrating that disruption of these pathways directly contributes to gliomagenesis [3, 4] In contrast, gliomas harboring *IDH* mutations are characterized by distinct, recurrent alterations, such as combinations of *IDH, TP53*, and *ATRX* mutations, or chromosomal 1p/19q co-deletion, which define a foundational genetic background; these molecular features play a central role in the diagnosis and prognostic stratification within the World Health Organization (WHO) 2021 classification of central nervous system tumors.

Across both *IDH*-wildtype and *IDH*-mutant gliomas, the acquisition of telomere maintenance mechanisms allows tumor cells harboring these driver genetic alterations to escape replicative senescence or crisis, thereby conferring cellular immortalization and enabling long-term tumor maintenance [5]. One such telomere maintenance mechanism is the acquisition of *TERT* promoter (*TERT*p) mutations. *TERT*p mutations enhance telomerase activity and elongate telomeres, thereby enabling cellular immortalization [6, 7]. Immortalized cells subsequently acquire additional alterations, ultimately leading to the development of detectable tumors [7, 8]. In GBM, *TERT*p mutations represent the most frequent genetic alterations, and two recurrent point mutations, c.-124C > T and c.-146C > T (hereafter referred to as C228T and C250T, respectively), have been reported with frequencies of approximately 70% for C228T and 30% for C250T [9, 10]. In oligodendrogliomas, *TERT*p mutations are observed in over 90% of cases, and unlike in GBM, *TERT*p C228T and C250T mutations are present at approximately equal frequencies [11]. *TERT*p mutations (C228T and C250T) are mutually exclusive,

indicating that either mutation alone is sufficient for tumor evolution [7, 9]. As a telomere maintenance mechanism distinct from *TERT*p mutations, astrocytomas, *IDH*-mutant predominantly rely on alternative lengthening of telomeres (ALT), often driven by the loss of ATRX [10]. Importantly, even in *TERT*p-wildtype GBM, genomic analyses have demonstrated that telomerase activation through TERT structural alterations and ALT phenotypes segregate into distinct molecular subgroups with strong mutual exclusivity [12]. Therefore, *TERT*p mutations, whether C228T or C250T, and ALT are considered to represent mutually exclusive mechanisms of telomere maintenance in diffuse gliomas.

Here, we report the first case of co-occurring *TERT*p mutations (both C228T and C250T) in a single GBM. We further characterized the molecular heterogeneity of this unique case through the use of patient-derived xenograft (PDX) models.

Materials and Methods

Study approval

This study was conducted in accordance with the Declaration of Helsinki and was approved by the Institutional Review Board of Yokohama City University (YCU, Yokohama, Japan; A171130006 and B190700012). Written informed consent was obtained from the patient and her family. All animal experiments were approved by the Animal Care and Use Committee of the YCU (approval number: FA25-007).

Histology

Tumor tissue specimens were fixed in 10% neutral-buffered formalin and embedded in paraffin. Hematoxylin and eosin staining was performed using standard procedures. For immunohistochemical staining, 5-μm–thick sections were deparaffinized, treated with 0.5% H_2O_2 in methanol, rehydrated, and heated for 20 min to facilitate antigen retrieval. After blocking with serum, tissue sections were incubated with the following primary antibodies: IDH1R132H [H09, Dianova GmbH (1:100), RRID: AB_2335716], ATRX [HPA001906, SIGMA (1:500), RRID: AB_1078249], p53 [DO7, DAKO (1:800), RRID: AB_322635], and Ki-67 (30 – 9, Roche Diagnostics, prediluted, RRID: AB_2631262).

Quantitative PCR assay

Quantitative polymerase chain reaction (qPCR) for the detection of *TERT* hotspot mutations C228T and C250T was performed as previously described [13]. Briefly, mutant-specific 5' nuclease probes combined with PNA/LNA clamping were used, with gene-specific PCR enzymes and master mixes. Assay sensitivity and variant allele frequency thresholds were evaluated using commercially available control DNA and genomic DNA from tumor cell lines harboring known mutations. Each run included both positive and negative controls. *CDKN2A* and *EGFR* copy numbers, and TERT mRNA expression were

assessed using SYBR Green–based qPCR and quantified by the ΔΔCt method. Primer sequences and detailed PCR conditions have been previously reported [13].

Genomic analysis

Genomic DNA was extracted from the tumor specimens using a commercially available kit (DNeasy Blood & Tissue Kit, Qiagen, Shanghai, China) according to the manufacturer's protocol. Multiplex ligation-dependent probe amplification (MLPA), methylation-specific polymerase chain reaction for O6-methylguanine methyltransferase (*MGMT*), and multiplex polymerase chain reaction (SNaPshot) were performed as previously described [14].

Digital PCR

A primer/probe mix for *TERT*p C228T/C250T was purchased from Integrated DNA Technologies, Inc. (Coralville, IA, USA). Droplets were generated and transferred to a 96-well plate, and the DNA was amplified using a thermal cycler. After PCR, the 96-well PCR plate was analyzed using a QX-200 droplet reader (Bio-Rad, Hercules, CA, USA), and the data were analyzed using the QX Manager 1.2 standard edition software (Bio-Rad). Mutation-specific signals were generated using a hexachlorofluorescein channel. Primer sequences and detailed PCR conditions have been previously reported [15].

Results

Case presentation

A 74-year-old woman (YMG247) presented with memory impairment and left hemiparesis. Her Karnofsky Performance Status (KPS) was 90. Magnetic resonance imaging (MRI) revealed a contrast-enhanced lesion in the right temporal lobe (Fig. 1A, left panel). A subtotal resection was performed, with residual tumor remaining in the posterior portion of the temporal lesion (Fig. 1A, middle panel). Histopathological examination revealed atypical glial cells with microvascular proliferation (Fig. 1B). Immunohistochemical staining showed a Ki-67 index of 18% (Fig. 1B). Therefore, the patient was diagnosed with GBM. The patient received focal radiation therapy (40 Gy in 15 fractions) with concomitant temozolomide and was discharged with a KPS of 90. However, local recurrence was detected 12 months postoperatively (Fig. 1A, right panel), and bevacizumab was administered. Unfortunately, the patient died 16 months after the initial diagnosis.

To analyze intratumoral genomic heterogeneity, we collected four distinct specimens from the contrast-enhanced lesion (Fig. 1C). Briefly, we assessed the genomic status of *IDH1* and *IDH2, TERT*p mutations, and *CDKN2A* homozygous deletions using our intraoperative integrated diagnostic system [13]. *IDH1* and *IDH2* mutations were not detected in any of the four multisampled specimens. Notably, concurrent *TERT*p C228T and C250T mutations were detected in all samples (Fig. 1D). The copy number of *CDKN2A*

showed loss in samples #1–3, while it was intact in sample #4. *EGFR* copy number was markedly amplified in sample #1 and amplified in sample #3, whereas it was intact in samples #2 and #4 (Fig. 1E). We also performed MLPA to validate copy number alterations and found amplification of *PDGFRA* and *EGFR* and loss of *CDKN2A* (Fig. 1F, Supplementary Fig. 1A). Digital PCR was performed to measure the variant allele frequency (VAF) of *TERT*p mutations in each sample. The results were as follows: in sample #1, the VAFs were 8.7% for C228T and 19.5% for C250T; in sample #2, they were 15.1% and 3.5%, respectively; in sample #3, they were 18.3% and 8.4%, respectively; and in sample #4, they were 10.9% and 23.4%, respectively (Fig. 1G). No clear association was observed between these copy number alterations and the VAFs of the respective *TERT*p mutations. Next-generation sequencing–based multiplex DNA analysis (MGH SnaPshot) confirmed dual *TERT*p mutations C228T (VAF 20%) and C250T *(*VAF 29%*)*, *EGFR* Arg108Lys (VAF 62%), and *TSHR* Arg450His (VAF 57%), with high-level amplification of *EGFR* and *MDM4* (Supplementary Fig. 1B). The tumor mutation burden was 5.4/Mb. TERT expression was comparable to that in other *TERT*p-mutant GBM cells (Supplementary Fig. 1C). *MGMT* promoter status was unmethylated (Supplementary Fig. 1D).

Patient-derived orthotopic xenograft model

To evaluate the potential for xenograft formation and subclonal evolution associated with dual *TERT*p mutations, we implanted patient tumor cells into the brains of female SCID-Beige mice. We confirmed the engraftment of tumor cells 117 days after implantation (YMG247-PDX). The tumor showed proliferating glial cells with atypical nuclei, which was consistent with the pathological findings of the patient tumor (Fig. 2A). Notably, qPCR analysis revealed that the tumor harbored only the *TERT* C228T mutation and lacked the C250T mutation (Fig. 2B). Digital PCR revealed that the PDX model harbored only the *TERT*p C228T mutation (VAFs were 50.3% for C228T and 0% for C250T, respectively; Fig. 2C). MLPA analysis demonstrated amplification of *PDGFRA* and *EGFR*, and loss of *CDKN2A* and *PTEN* in the xenograft tumors (Fig. 2D, Supplementary Fig. 2). Importantly, these copy number alterations (CNAs) were more extensive compared to the original patient tumor, indicating subclonal selection of cells harboring the *TERT*p C228T mutation and multiple CNAs during *in vivo* tumor propagation.

Discussion

This case provides the first evidence of a GBM harboring dual *TERT*p mutations within a single tumor. Because these mutations are generally regarded as mutually exclusive, their coexistence across multiple tumor regions suggests intratumoral heterogeneity. Furthermore, the availability of a PDX model enabled functional validation of this unique genomic profile. Notably, only the *TERTp* C228T mutation was retained in the PDX tumors, indicating subclonal selection during tumor propagation.

*TERT*p mutations are observed in approximately 55–70% of GBMs, are generally maintained at recurrence, and are considered to be acquired at an early stage of tumorigenesis [16, 17, 18]. However, evolutionary dynamics analyses of paired initial and recurrent GBM samples have demonstrated that

copy number variations in chromosomes 7, 9, and 10 occur early in tumorigenesis, whereas *TERT*p mutations are subsequently acquired through subclonal evolution [7]. In the present study, both *TERT*p C228T and C250T mutations were present in the same specimen, whereas only C228T was retained in the PDX model. This suggests that *TERT*p C228T- and C250T–harboring cells coexist as subclones within the same tumor specimen at the bulk-tumor level, supporting a model in which *TERT*p mutations represent delayed subclonal events rather than early truncal events in the present case.

In most previous studies, *TERT*p mutations C228T and C250T have been collectively classified as "*TERT* promoter mutations," and potential biological or clinical differences between these two variants have not been sufficiently investigated. In the present case, because no clear association was observed between *EGFR* or *CDKN2A* copy number alterations and the VAFs of individual *TERT*p mutations at the bulk level, it cannot be concluded that either *TERT* C228T or C250T mutation is more strongly involved in the acquisition of driver alterations. Addressing this question will require single-cell–level analyses to resolve subclonal relationships. In contrast, in the patient-derived xenograft tumor, only the *TERT*p C228T mutation was retained, concomitant with more extensive copy number alterations, including *EGFR* amplification and *CDKN2A* loss. These findings raise the possibility that *TERT*p C228T-mutant cells possess a selective advantage, potentially facilitating the acquisition of additional driver alterations, although species-specific effects cannot be excluded (Fig. 2E). In the clinical setting of GBM, the frequencies of *TER*Tp C228T and C250T are approximately 70% and 30%, respectively. Only C228T has been reported to be associated with poorer clinical outcomes [18]. In papillary thyroid carcinoma, tumors harboring the *TERT*p C228T mutation have been shown to exhibit a more pronounced increase in TERT mRNA expression than those carrying the C250T mutation and are more strongly associated with aggressive clinicopathological features and worse prognosis [19]. From a mechanistic perspective, although both *TERT*p mutations generate a de novo E-twenty-six (ETS) transcription factor binding site (CCTT) within *TERT*p, differences in their promoter locations may influence the efficiency of transcriptional complex assembly and modulate crosstalk with other signaling pathways, such as NF-κB [20, 21]. Collectively, these observations suggest that *TERT*p C228T and C250T mutations may not be functionally equivalent, with C228T potentially conferring a modestly stronger telomerase-activating effect in certain biological contexts.

In large GBM cohorts in which *TERT*p mutations C228T and C250T were reported separately, no cases harboring both mutations were identified concurrently, except for a single case among 144 patients (0.69%) reported by Nonoguchi et al. However, in that report, no further clinical or molecular details, including *IDH* mutation status, were provided, limiting interpretability [10, 11, 18, 22]. In contrast, Arita et al. reported four cases (1.4%) of concurrent *TERT*p C228T and C250T mutations in 279 oligodendroglioma cases [11]. Notably, in *IDH*-mutant gliomas, *TERT*p mutations are generally associated with a favorable prognosis, suggesting that the biological role of TERT activation may differ substantially between *IDH*-wildtype and *IDH*-mutant gliomas [11].

In summary, this report provides the first detailed molecular characterization of an *IDH*-wildtype GBM harboring both *TERT*p C228T and C250T mutations, together with xenograft experiments demonstrating

their subclonality and evolutionary dynamics, as evidenced by the selective retention of *TERT*p C228T during patient-derived xenograft passaging. This case highlights the importance of considering telomere maintenance as a dynamic, heterogeneous process in GBM rather than a fixed early oncogenic event.

Declarations

Acknowledgments

The authors thank Ms. Miyu Okura, and Mr. Ye Weikai (Yokohama City University) for technical assistance.

Conflict of interest

The authors declare no conflicts of interest related to this study.

Financial Support:

This work was supported by Grant-in-Aid for Scientific Research (22K09210), Strategic Research Promotion of Yokohama City University research, and Yokohama Foundation for Advancement of Medical Science (to KT).

References

1. Stupp R, Taillibert S, Kanner A et al (2017) Effect of Tumor-Treating Fields Plus Maintenance Temozolomide vs Maintenance Temozolomide Alone on Survival in Patients With Glioblastoma: A Randomized Clinical Trial. JAMA 318(23):2306–2316
2. Cancer Genome Atlas Research N (2008) Comprehensive genomic characterization defines human glioblastoma genes and core pathways. Nature 455(7216):1061–1068
3. Koga T, Chaim IA, Benitez JA et al (2020) Longitudinal assessment of tumor development using cancer avatars derived from genetically engineered pluripotent stem cells. Nat Commun 11(1):550
4. Miki S, Koga T, McKinney AM et al (2022) TERT promoter C228T mutation in neural progenitors confers growth advantage following telomere shortening in vivo. Neuro Oncol 24(12):2063–2075
5. Barthel FP, Wesseling P, Verhaak RGW (2018) Reconstructing the molecular life history of gliomas. Acta Neuropathol 135(5):649–670
6. Chiba K, Lorbeer FK, Shain AH et al (2017) Mutations in the promoter of the telomerase gene TERT contribute to tumorigenesis by a two-step mechanism. Science 357(6358):1416–1420
7. Korber V, Yang J, Barah P et al (2019) Evolutionary Trajectories of IDH(WT) Glioblastomas Reveal a Common Path of Early Tumorigenesis Instigated Years ahead of Initial Diagnosis. Cancer Cell 35(4):692–704 e12
8. Sanchez-Vega F, Mina M, Armenia J et al (2018) Oncogenic Signaling Pathways in The Cancer Genome Atlas. Cell 173(2):321–337 e10

9. Arita H, Narita Y, Fukushima S et al (2013) Upregulating mutations in the TERT promoter commonly occur in adult malignant gliomas and are strongly associated with total 1p19q loss. Acta Neuropathol 126(2):267–276
10. Killela PJ, Reitman ZJ, Jiao Y et al (2013) TERT promoter mutations occur frequently in gliomas and a subset of tumors derived from cells with low rates of self-renewal. Proc Natl Acad Sci U S A 110(15):6021–6026
11. Arita H, Matsushita Y, Machida R et al (2020) TERT promoter mutation confers favorable prognosis regardless of 1p/19q status in adult diffuse gliomas with IDH1/2 mutations. Acta Neuropathol Commun 8(1):201
12. Diplas BH, He X, Brosnan-Cashman JA et al (2018) The genomic landscape of TERT promoter wildtype-IDH wildtype glioblastoma. Nat Commun 9(1):2087
13. Hayashi T, Tateishi K, Matsuyama S et al (2024) Intraoperative Integrated Diagnostic System for Malignant Central Nervous System Tumors. Clin Cancer Res 30(1):116–126
14. Tateishi K, Nakamura T, Juratli TA et al (2019) PI3K/AKT/mTOR Pathway Alterations Promote Malignant Progression and Xenograft Formation in Oligodendroglial Tumors. Clin Cancer Res 25(14):4375–4387
15. On J, Natsumeda M, Takahashi H et al (2024) Reliable detection of genetic alterations in cyst fluid DNA for the diagnosis of brain tumors. J Neurooncol 166(2):273–282
16. Abou-El-Ardat K, Seifert M, Becker K et al (2017) Comprehensive molecular characterization of multifocal glioblastoma proves its monoclonal origin and reveals novel insights into clonal evolution and heterogeneity of glioblastomas. Neuro Oncol 19(4):546–557
17. Makino R, Bajagain M, Higa N et al (2025) Analysis of clinical, histological, and genomic information of molecular glioblastoma in a Japanese glioma cohort. Brain Tumor Pathol 42(3):68–75
18. Nonoguchi N, Ohta T, Oh JE et al (2013) TERT promoter mutations in primary and secondary glioblastomas. Acta Neuropathol 126(6):931–937
19. Marczyk VR, Maia AL, Goemann IM (2024) Distinct transcriptional and prognostic impacts of TERT promoter mutations C228T and C250T in papillary thyroid carcinoma. Endocr Relat Cancer. ;31(9)
20. Li Y, Zhou QL, Sun W et al (2015) Non-canonical NF-kappaB signalling and ETS1/2 cooperatively drive C250T mutant TERT promoter activation. Nat Cell Biol 17(10):1327–1338
21. Bell RJ, Rube HT, Kreig A et al (2015) Cancer. The transcription factor GABP selectively binds and activates the mutant TERT promoter in cancer. Science 348(6238):1036–1039
22. Brennan CW, Verhaak RG, McKenna A et al (2013) The somatic genomic landscape of glioblastoma. Cell 155(2):462–477

Figures

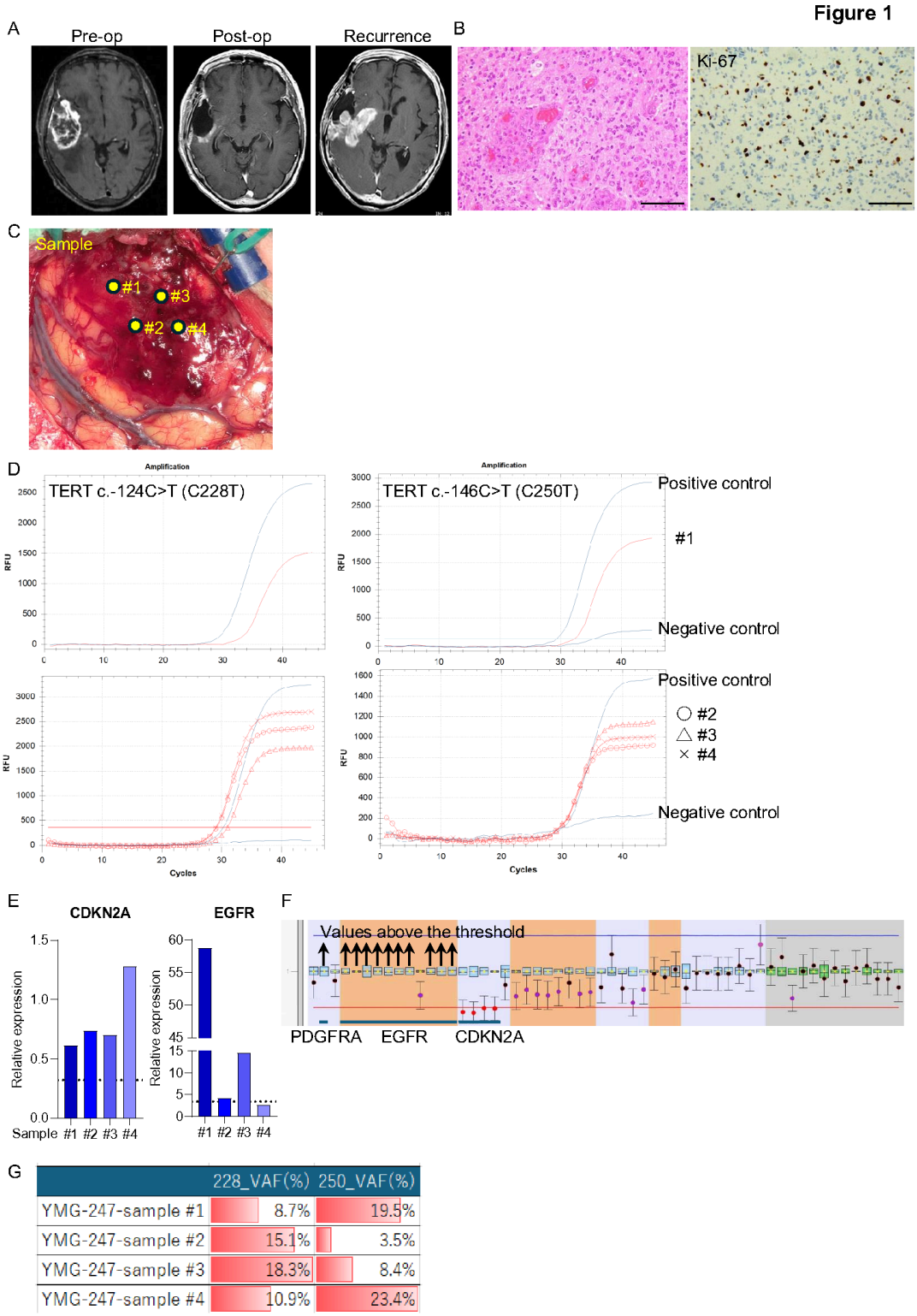


Figure 1

Characteristics of the primary tumor (YMG247). (A) Contrast-enhanced magnetic resonance images. Left panel, preoperative; middle panel, postoperative; right panel, recurrent disease. (B) Hematoxylin and eosin staining, and immunohistochemical staining for Ki-67 (scale bar = 100 μm). (C) Intraoperative photograph showing the sampling sites. (D) Quantitative PCR (qPCR) analysis for *TERT* promoter mutations C228T (left) and C250T (right). (E) qPCR analysis of copy number alterations in *CDKN2A* and

EGFR. (F) Multiplex ligation-dependent probe amplification (MLPA) analysis assessing copy number alterations in *PDGFRA, EGFR, CDKN2A, PTEN, CDK4, MDM2*, and *TP53*. Genes showing copy number alterations are annotated. (G) Digital PCR analysis of variant allele frequencies of *TERT* promoter mutations in each sample.

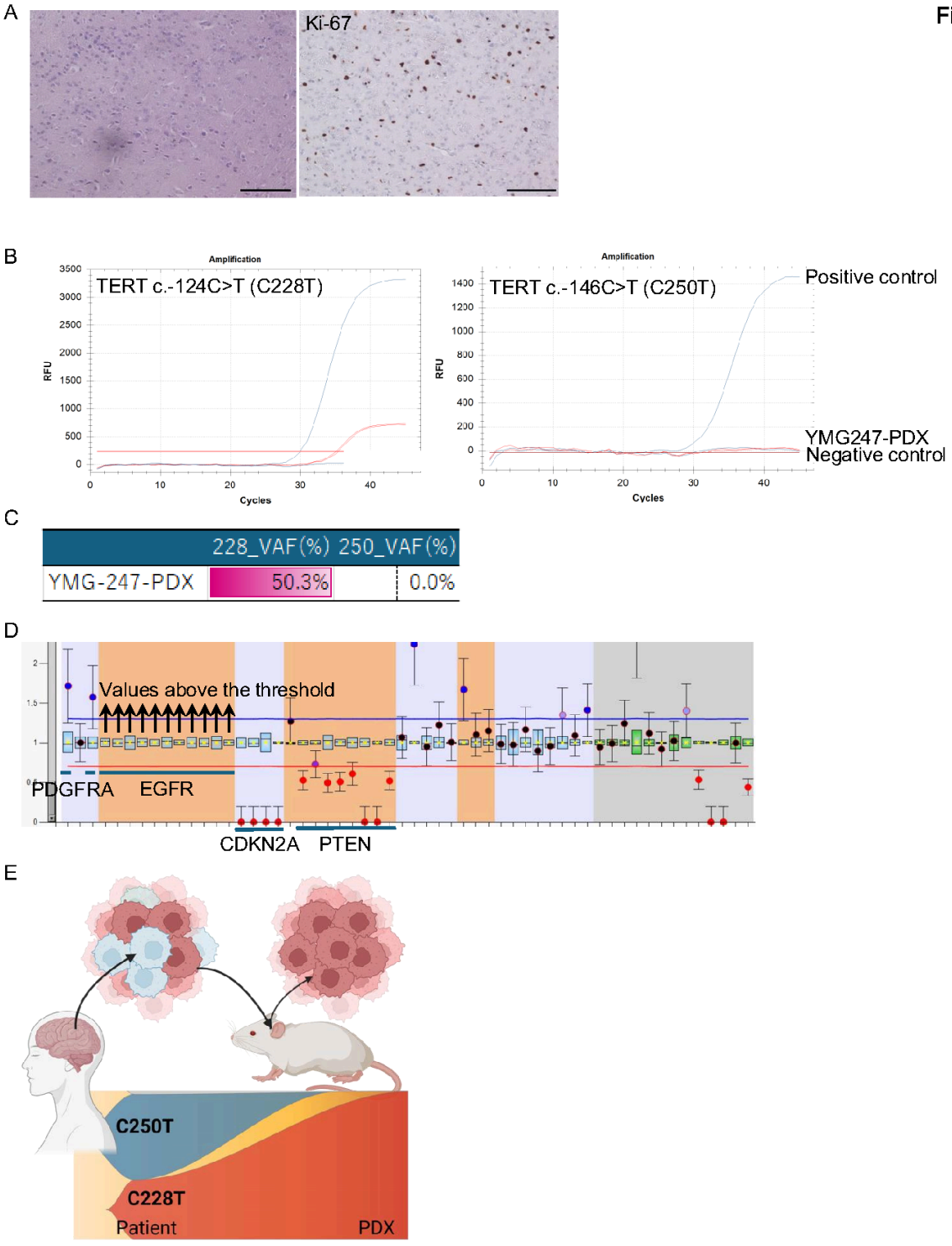


Figure2

Figure 2

Characteristics of the patient-derived orthotopic xenograft model (YMG247-PDX). (A) Hematoxylin and eosin staining and immunohistochemical staining for Ki-67 (scale bar = 100 μm). (B) qPCR analysis for *TERT*promoter mutations C228T (left) and C250T (right). (C) Digital PCR analysis of variant allele frequencies of *TERT* promoter mutations. (D) MLPA assessing copy number alterations in *PDGFRA, EGFR, CDKN2A, PTEN, CDK4, MDM2*, and *TP53*. Genes showing copy number alteration are annotated. (E) Schematic representation of subclonal selection in the patient tumor and the patient-derived xenograft (PDX) tumor.

Supplementary Files

This is a list of supplementary files associated with this preprint. Click to download.

- Supplementaryfigure.pdf